INTERNATIONAL JOURNAL OF HYDROGEN ENERGY 33 (2008) 5589–5595

Available at www.sciencedirect.com

ScienceDirect

journal homepage: www.elsevier.com/locate/he

Mathematical modelling of UH_3 formation

Ilya A. Chernov[a,*], *Joseph Bloch*[b], *Igor E. Gabis*[c]

[a]*Institute of Applied Mathematical Research, Karelian Research Centre of RAS, Pushkinskaya 11, 185910 Petrozavodsk, Russia*
[b]*Nuclear Research Center-Negev, P.O. Box 9001, Beer Sheva 84190, Israel*
[c]*V.A. Fock Institute of Physics, St. Petersburg State University, 198504, Russia*

ARTICLE INFO

Article history:
Received 25 September 2007
Received in revised form
9 June 2008
Accepted 9 June 2008
Available online 17 September 2008

Keywords:
Hydride formation
Mathematical modelling
Isothermal hydriding
Uranium hydride
Evaluating the kinetic constants

ABSTRACT

In this paper we develop the mathematical model for the kinetics of isothermal hydriding of metal powders under constant low (near equilibrium) pressures. We consider four successive stages of hydriding: nucleation, skin development, skin growth, and final saturation. Each stage is described by its own equations derived from the mass conservation law. Our approach is to consider a few concurrent processes instead of choosing a single limiting one. We used the model to approximate the series of experimental curves (for successive cycles of hydriding of uranium) and obtained some evaluations for the kinetic parameters.

1. Introduction

Understanding the hydriding kinetics of powder particles is very important for energy storage applications [1]. According to the US Department of Energy objectives, loading of a hydrogen vehicle tank by 2010 must not exceed 3 min. This implies not only heat problems but also serious limitations on rate of hydrogen sorption by metal hydride powder. Existing articles give contradictory information about sorption and its limiting factors. The data for uranium we have obtained allow to study the sorption in detail and to get the evaluations of the rate constants. This procedure could also be applied for other, more important from the practical point of view, hydrides of metals.

The hydriding kinetics is quite difficult to simulate. There have been many attempts to present models simulating the penetration of hydrogen into a particle [2]. In the simplest models the experimental results were analyzed according to a single equation (e.g. a first order or the Johnson–Mehl equations). More complex models were based on a series of consecutive steps by which hydrogen is penetrating into the particle [2,3]. However, the real case is even more complex: it has been shown [4] that for the most general case the hydriding reaction of a metal particle consists of several partially separated stages such as: the penetration of hydrogen through the surface passivation layer and the build-up of hydrogen concentration in the metal-oxide interface, the nucleation and growth stage which precedes the hydride phase layer formation on the particle's surface, and the advance of the hydride layer (the skin) into the particle interior. Other possible stages are the dissolution of H in the hydride phase (saturation) and the formation of higher hydrides. In this work we adopt this point of view to construct a mathematical model for the time dependent hydrogen absorption in a metallic particle forming a single hydride phase. We neglect the surface passivation layer effects. This is

* *Corresponding author*. Tel.: +7 9212227447; fax: +7 8142766313.
E-mail addresses: iachernov@yandex.ru, chernov@karelia.ru (I.A. Chernov).
0360-3199/$ – see front matter © 2008 International Association for Hydrogen Energy. Published by Elsevier Ltd. All rights reserved.
doi:10.1016/j.ijhydene.2008.06.070

justified for the special case of activated metal powders. The model includes four successive stages: nucleation, growth of the nuclei to form a skin layer, the advance of the skin into the particle, and the final saturation. The model is applied for several successive hydriding cycles of uranium under relatively low pressures.

2. The model

2.1. The model assumptions

We consider a single powder particle. Its form is approximated by sphere and cylinder. In case of cylinders they are assumed to be long and thin so that the butts could be neglected. In both cases we consider the hydride skin on the core of pure metal. This core has the same form as the particle, i.e. spherical core in spherical particles, cylindrical core (of smaller radius but of the same height) in cylindrical ones. Note that length of cylinders is not important for the relative quantities such as fractions of the hydride phase or of the sorbed hydrogen. By ''hydride'' we mean hydride phase with some dissolved hydrogen (so concentration may be above stoichiometric).

As is written in Ref. [4], due to the higher activation energy of the diffusion through the hydride compared with the overall kinetics in bulk samples (for which the penetration is through the metal), one can say the diffusion through the hydride is slower compared with that through the metal. So we assume that the diffusion in the hydride is rather slow compared to the diffusion in the metal and consider only the first and not the second (fast diffusion). Besides, we neglect the concentration in the metal (considering it is small compared to that in hydride).

The hydrogen pressure and the sample's temperature are considered to be constant (due to the experimental conditions). The particle size is assumed to be constant during the hydriding cycle, but it decreases from one cycle to another because the powder becomes finer. We suppose only spherical or cylindrical symmetry for the particles.

Let D be the Fick's diffusivity in hydride, and $c(t,r)$ is the hydrogen concentration distribution there. Here r is the radius in spherical or cylindrical coordinate system. Due to the mentioned symmetry the concentration is independent of the angle variables. Let L be the radius of the particle. The cylinder's length is not important for the results. The radius of the metal core under the hydride skin is denoted by $\rho(t)$. When all the surface of the particle is covered by the new hydride phase this radius is denoted by ρ_0. Let S and V be the surface area (the lateral surface in case of a cylinder) and volume of the particle, respectively.

The stoichiometric hydrogen concentration in hydride is denoted by $\bar{c}$. Note that the concentration in the hydride can exceed stoichiometric, i.e. some hydrogen can dissolve and diffuse in the hydride. Thus, the modelled quantity is the amount of absorbed hydrogen.

The flux of hydrogen sorption by hydride is the result of counteraction of the absorption flux and the desorption flux. The desorption flux density is described by $J_{\mathrm{des}} = bc^2(t,L)$. Here b is the desorption rate constant. Quadratics in the formula is the result of the fact that two atoms form one H_2 molecule. The absorption flux density J_{abs} is constant due to the constant pressure and temperature. The pressure dependence of J_{abs} is not considered. The resulting net flux density is $J_\beta = J_{\mathrm{abs}} - bc^2(t,L)$.

The flux density J_α of hydrogen absorption by the metal is defined in a similar way. But densities of absorption and desorption fluxes for the metal are not considered separately, only their difference J_α is considered.

We suggest the following four-stage scenario for the hydriding process. (a) The nucleation stage, during which nuclei growth is limiting. (b) The hydride skin formation; we model its growth by symmetrical nuclei. Here absorption becomes the most important. (c) After the skin has been completed, it becomes thicker due to hydrogen absorption and diffusion towards the phase boundary. (d) Finally, after the entire particle has transformed into hydride, it saturates with hydrogen up to the equilibrium concentration. Now, let us consider in detail the models for these stages. We present formulae for spherical shape only. For cylinders the formulae are similar.

2.2. Nucleation

Let us consider the very beginning of the experiment, when the first new-phase nuclei appear. They use hydrogen around them to grow; the concentration drop is small and is compensated by fast diffusion and absorption. Nucleation is a limiting step.

The total volume and surface of the nuclei are denoted by v and s, respectively. We assume that the concentration in the hydride nuclei is constant, so the amount G of hydrogen in the nuclei is proportional to v. We suggest that the geometrical shape and the number of the nuclei do not change during the process, so approximately s^3 is proportional to v^2. Tiny nuclei appear and hydrogen dissolved around them is absorbed through their total surface. Sorption on the sample's surface provides exactly as much hydrogen as the nuclei need. Due to the conservation law dG is proportional to sdt. Using the initial condition $v(0) = 0$ we finally obtain

$$G(t) = \lambda t^3, \quad 0 \le t \le t_\lambda. \tag{1}$$

The factor λ contains information about the geometric shape, number of the nuclei, concentration there, etc. This kinetic behaviour is characteristic of the initial stages of solid-state nucleation and growth processes, prior to overlapping (The Johnson–Mehl equation for $\lambda t^3 << 1$). This model works well while nucleation is strictly the limiting step (up to t_λ). Later, when nuclei have become large enough, their growth needs more hydrogen than is around them; thus sorption becomes a limiting step: firstly sorption by the metal, later also sorption by the hydride, after the hydride has got its own hydrogen-facing surface.

This stage is described by two parameters: λ and t_λ, i.e. the nucleation constant and the time of nucleation. During this stage nucleation is the limiting step.

2.3. Skin development

It is difficult to describe in detail the realistic formation of the skin by the growing nuclei of the new hydride phase due to complex shape of the nuclei and their growth and overlap.

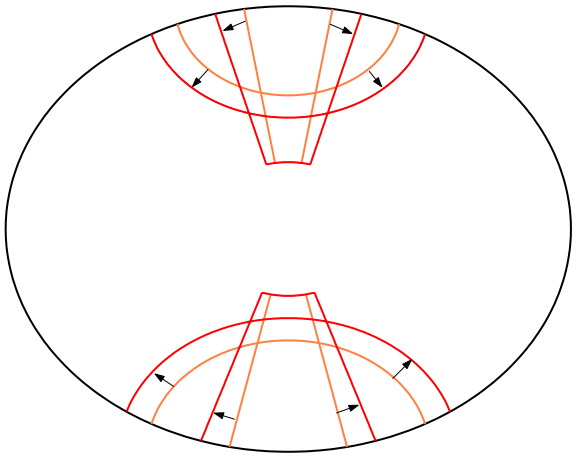

Fig. 1 – Real and model nuclei.

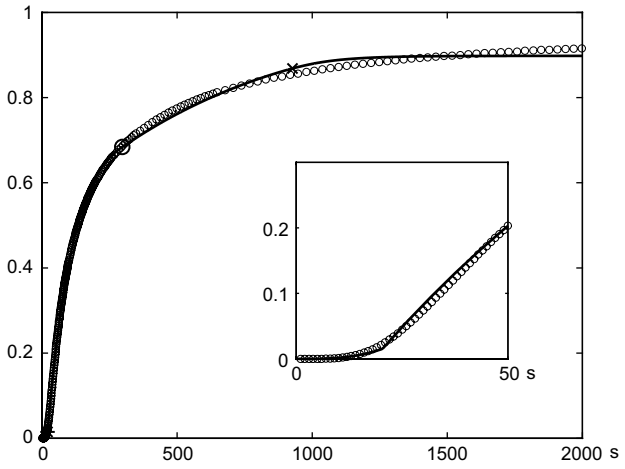

Fig. 3 – Second cycle, cylindrical powder particles.

Hydrogen concentration in the nuclei is not constant. We model the nuclei by symmetrical geometrical objects for the sake of reasonable simplicity. The symmetry is with respect to the appropriate curvilinear coordinate system (spherical one in our case). Our model nuclei are compared to "more real" ones in Fig. 1. A good photo of a nucleus can be found in Ref. [5]. Real nuclei are round; their growth is increase of radii. The model nuclei are symmetrical objects; their growth is conceived by the increase of solid angles. A nucleus is at any spot on the surface and is formed by parts of all spherical radii from ρ_0 to L. The nuclei occupy the spherical layer between two spheres and are formed by radii. To obtain an expression for the absorbed amount of hydrogen at this stage we need an equation for the area $S_\beta(t)$ under all the nuclei of the new phase on the surface of the particle. Spatial concentration distribution in the nuclei is assumed to be stationary (and hence, time independent). In spherical coordinates it is a hyperbola $c(t,r) = A + B/r$. The constant coefficients A and B are obtained from the boundary conditions. These are the stoichiometric concentration in the hydride on the phase boundary: $c(t,\rho_0) = \bar{c}$, and the flux balance on the surface: $J_\beta = D(\partial c/\partial r)(t,L)$. These conditions yield the quadratic equation for B:

$$b(L-\rho_0)^2B^2 - \left(2b\bar{c}(L-\rho_0)L\rho_0 + D\rho_0^2\right)B - L^2\rho_0^2\left(J_{abs} - b(\bar{c})^2\right) = 0. \tag{2}$$

As absorption is greater than desorption, the free term is negative and thus the equation has a positive and a negative root. Obviously $B<0$ so we use the negative one. So A and B are determined uniquely.

The amount of hydrogen in the nuclei with total area $S_\beta(t)$ is

$$\frac{S_\beta(t)}{S}\int_{\rho_0}^{L} c(t,r)4\pi r^2 dr = \frac{S_\beta(t)}{L^2}\int_{\rho_0}^{L}\left(A+\frac{B}{r}\right)r^2 dr = S_\beta(t)\left(A\frac{L^3-\rho_0^3}{3L^2} + B\frac{L^2-\rho_0^2}{2L^2}\right). \tag{3}$$

W denotes the constant factor in the brackets. It describes the geometry and the stationary distribution (obviously it is different for cylinders). The increase of the total amount equals the sorbed quantity. Thus we have the differential equation:

$$W\frac{d}{dt}S_\beta = J_\beta S_\beta(t) + J_\alpha(S - S_\beta(t)), \quad S_\beta(t_\lambda) = 0, \quad t \geq t_\lambda. \tag{4}$$

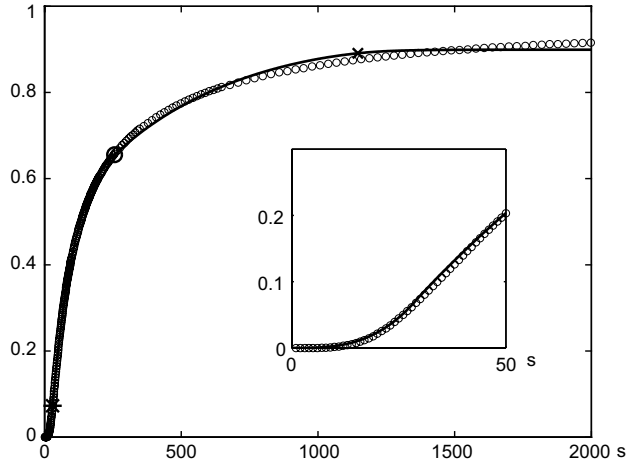

Fig. 2 – Second cycle, spherical powder particles.

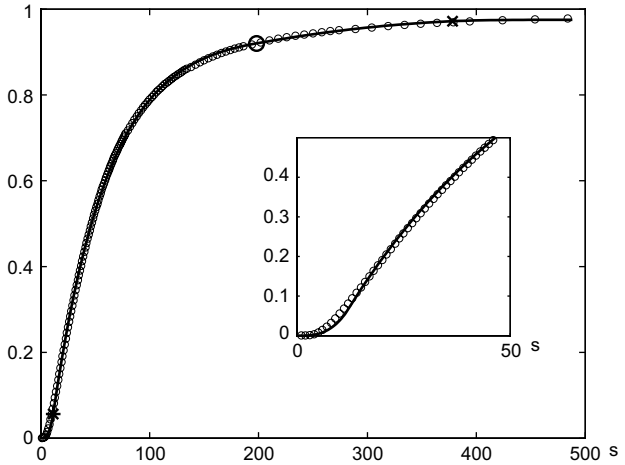

Fig. 4 – Sixth cycle, spherical powder particles.

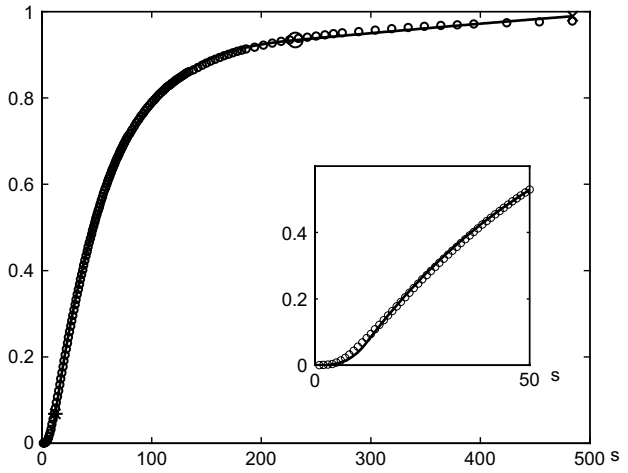

Fig. 5 – Sixth cycle, cylindrical powder particles.

Since the temperature, pressure, and skin width are constant, this equation is solved explicitly:

$$S_\beta(t) = \frac{J_\alpha S}{J_\alpha - J_\beta}\left(1 - \exp\left(-\frac{J_\alpha - J_\beta}{W}(t - t_\lambda)\right)\right), \quad t \geq t_\lambda. \tag{5}$$

The absorption of hydrogen by the metal should be greater than that by the hydride, therefore $J_\alpha > J_\beta$. The function $S_\beta(t)$ reaches the value S by finite time

$$t = t_\lambda + W\frac{\ln(J_\alpha) - \ln(J_\beta)}{J_\alpha - J_\beta}. \tag{6}$$

We assume that a skin of constant width ρ_0 is ready when all the surface of the particle is covered by the new phase. This width ρ_0 is a parameter to be determined. The skin may occupy a significant part of the particle's volume. The registered quantity is G(t), $dG = (J_\alpha(S - S_\beta) + J_\beta S_\beta)dt$.

2.4. *Skin growth*

Once the hydride skin is complete hydrogen is still absorbed by the hydride surface since its pressure is above equilibrium. This means that hydrogen concentration near the surface is above stoichiometric; hydrogen diffuses to the phase boundary and is used for hydride formation, so the border line is moving. Obviously the concentration on the phase boundary is always stoichiometric. The boundary advance is described by the conservation law: all the hydrogen arriving at the phase boundary is used for hydride formation. Due to the symmetry we can mathematically describe this process by the Stefan-type single-dimension diffusion boundary-value problem with moving boundary:

$$\frac{\partial c}{\partial t} = D\left(\frac{\partial^2 c}{\partial r^2} + \frac{2}{r}\frac{\partial c}{\partial r}\right), \quad r \in (\rho(t), L), \quad t \in (t, t^{**}), \tag{7}$$

Table 1 – Diffusivity D in UH_3 (10^{-16} m^2 s^{-1})

Cycle no.	2	3	4	5	6	7	Many
Spheres	7.2643	7.7077	7.1574	10.698	9.7852	7.1676	6.4050
Cylinders	7.4455	7.7583	7.1504	11.065	8.6609	8.5953	8.0048

Table 2 – Desorption from UH_3 rate constant b (10^{-35} m^4 s^{-1})

Cycle no.	2	3	4	5	6	7	Many
Spheres	1.5437	1.5190	1.8661	1.7181	1.7745	1.8997	1.9512
Cylinders	1.5275	1.3666	1.7563	1.6187	1.8862	1.6457	1.6685

$$J_\beta(t) = J_{abs} - bc^2(t, L) = D\frac{\partial c}{\partial r}(t, L), \tag{8}$$

$$c(t, \rho(t)) = \bar{c}, \tag{9}$$

$$\bar{c}\frac{d\rho}{dt} = -D\frac{\partial c}{\partial r}(t, \rho(t)), \quad \rho(t) = \rho_0, \tag{10}$$

$$c(t^*, r) = A + \frac{B}{r}, \quad r \in [\rho_0, L]. \tag{11}$$

Eq. (7) is the diffusion equation in spherical coordinates. At time t^{**} the metal phase disappears, i.e. $\rho(t^{**}) = 0$. By this stage the particle is fully hydrided. Eq. (8) is the flux balance on the surface. Next comes the condition of stoichiometric concentration on the phase boundary Eq. (9) and the conservation on the moving boundary Eq. (10) (the Stefan-type condition). Finally there are initial data Eq. (11). This boundary-value problem is the most difficult for solution because of nonlinearity and moving boundary. The registered quantity is $G(t)$, $dG = J_\beta(t)Sdt$.

2.5. *Final saturation*

At the final stage of the process the reaction is slowed down. We assume that the particle consists of hydride that can sorb hydrogen. The mathematical model is the boundary-value problem similar to Eqs. (7)–(11), only now $\rho(t) = 0$ (no metal) and boundary condition Eq. (9) is replaced by the condition of spherical symmetry that is Eq. (10) with $\rho(t) = 0$. The initial data $c(t^{**}, r)$ are taken from the solution to the previous problem (instead of Eq. (11)). The stop moment t_{end} is chosen arbitrarily. Theoretically, infinite time is needed to reach the precise equilibrium with respect to the pressure.

c_{eq} denotes the equilibrium concentration. Equilibrium means that $J_\beta = 0$ and thus

$$c_{eq} = \sqrt{\frac{J_{abs}}{b}}. \tag{12}$$

If the entire particle consists of hydride with this equilibrium concentration, it contains $G_{lim} = c_{eq}V$ hydrogen atoms.

Table 3 – Density of flux of hydrogen absorption by UH_3 (10^{23} m^{-2} s^{-1})

Cycle no.	2	3	4	5	6	7	Many
Spheres	1.4339	1.4866	1.4281	1.5123	1.3943	1.4013	1.3617
Cylinders	1.4894	1.5182	1.5451	1.8581	1.3869	1.2277	1.1618

Table 4 – Difference between densities of sorption and desorption by U (10^{20} m^{-2} s^{-1})

Cycle no.	2	3	4	5	6	7	Many
Spheres	2.3874	2.4315	2.2243	2.1471	2.6492	2.4725	0.8724
Cylinders	2.2422	3.5524	4.1715	3.1321	3.7231	3.7819	1.1458

We still register the amount $G(t)$ of absorbed hydrogen: $dG = J_\beta(t)Sdt$

The fraction of hydrogen absorbed by the time t is

$$g(t) = \frac{G(t)}{G_{lim}}, \quad t \geq 0. \tag{13}$$

The function $g(t)$ is the quantity actually measured by time t during the kinetic experiment.

3. Applying the model to the system U–UH_3

3.1. The experiment

The experiments were performed in a quartz constant-volume Sieverts system [6]. Samples of machined chips of uranium – 0.1 wt% Cr – were placed inside an alumina crucible. The crucible was inserted in a quartz reactor equipped with a thermocouple. The reactor was then attached to the P–V–T system. An additional buffer volume was attached to the reaction cell through a separation valve. Its purpose was to restore the hydrogen working pressure to its initial value whenever the pressure drop exceeds 5% of the initial pressure. The time dependence of the hydrogen pressure $P(t)$ was followed using a capacitance pressure transducer. Time, pressure, and temperature were recorded in a data file using a data acquisition arrangement. The details of the experimental system and procedure are further described in Ref. [6]. The model assumptions about constant pressure and temperature are justified by the experimental conditions. Phase diagram for U can be found in Ref. [7]. We used six experimental curves for successive hydriding cycles and one after a large number of cycles, all obtained for 370 °C (603 K).

3.2. The adjusted parameters

To fit the experimental data we have used the least squares method. Nine parameters to be determined were: the density J_{abs} of hydrogen absorption by UH_3 and the rate constant b for desorption from UH_3; difference J_α between absorption and desorption by U; the diffusivity D in UH_3; the mean radius L of the particles (radius of the base for cylinders); the relative width of the initial skin $1-\rho_0 L^{-1} > 0$; the nucleation constant λ and the nucleation time t_λ; the scale factor m, which describes the real unit level. Probably the unit level in the experimental plots is not the real unit level, i.e. the concentration at these times is not equilibrium, because the gradient of the experimental curves is not zero at the most right point. Notice that we do not consider desorption and absorption by U separately, only their difference is studied; also notice that the diffusion in U is very fast compared to that in hydride.

Table 6 – Initial relative volume of the hydride skin $(1-(V(\rho_0)/V(L)))100$

Cycle no.	2	3	4	5	6	7	Many
Spheres	74.609	87.049	82.254	97.828	95.572	90.541	77.355
Cylinders	80.548	89.471	85.017	45.131	84.461	91.805	78.236

3.3. Fitting the experimental data by the model curves

Figs. 2–5 compare the experimental curves and the fitted model curves. They are fraction of adsorbed hydrogen with respect to time. Unit level corresponds to stoichiometric concentration in the whole particle. The nucleation time t_λ, the time t when the skin is ready, and the time t^{**} when the final saturation starts are denoted by an asterisk, a circle, and a cross, respectively. The first 50 seconds of each process are shown in the insert in each plot in order to better observe the nucleation stage. Figs. 2 and 4 show the results for the spherical particles; Figs. 3 and 5 are for the cylindrical particles.

The deviations of the model-based curves from the experimental data shown in Figs. 2–5 are the result of the difference in size and shape between the real and the modelled particles. The model was constructed under assumption that the particles are equivalent, and this difference must somehow smooth the results.

The parameters for different cycles are presented in Tables 1–9.

One can see that absorption flux densities, the diffusivity, and the desorption rate constant vary a little from cycle to cycle and are similar for spherical and cylindrical shape, as expected. Particle radius decreases from cycle to cycle. This means that the powder becomes finer.

The nucleation constant λ is the amount of hydrogen taken by the nuclei during the first second. Dividing it by the particle's surface $S(L)$, we obtain the amount of hydrogen absorbed by a unit surface during the first second. The parameter λ increases and t_λ decreases with increasing number of cycles. This shows that some hydrogen is left in the particle after the decomposition, so that during the next cycle there is more hydrogen after the first second of hydriding. Thus the nucleation goes faster and becomes nonlimiting at an earlier stage. The effect of the nucleation parameters is limited to the very

Table 5 – Radius L of the particle (10^{-7} m)

Cycle no.	2	3	4	5	6	7	Many
Spheres	8.6913	8.4421	5.3707	5.2167	4.6877	4.6818	2.4091
Cylinders	7.8692	7.7599	6.5214	5.4094	5.2453	4.8797	1.9307

Table 7 – Scale factor m (dimensionless)

Cycle no.	2	3	4	5	6	7	Many
Spheres	0.8151	0.7874	0.8586	0.9509	0.9116	0.9212	0.9451
Cylinders	0.8800	0.7893	0.8455	1.1490	1.0316	0.9320	0.9457

Table 8 – Relative nucleation constant $\lambda S(L)^{-1}$ (10^{17} m^{-2} s^{-3})

Cycle no.	2	3	4	5	6	7	Many
Spheres	1.0059	1.7294	2.9891	2.9849	5.8107	5.2586	76.280
Cylinders	0.8033	2.5913	9.4946	4.5411	8.6268	9.4139	23.793

beginning of the hydriding process, making their fitted values less reliable than the other parameters. The aim of this part of the model is only to explain the S-shape of the experimental curves by a physically reasonable scenario. One can see that due to the nucleation stage the curves are S-shaped, in accordance with the experimental data.

The scale factor m changes from one cycle to another because the unit level is naturally different for each cycle. For spherical and cylindrical particles the scale factor m is almost the same for each separate cycle. This proves that m really is the real unit level for each separate experiment.

The mean particle radius L is very important. In fact, we can define only how L changes from cycle to cycle; the initial radius has been determined based on the micrograph shown in Ref. [6].

Note that the relative volume of the hydride skin (at the moment it has just appeared) is, in general, similar for spherical and cylindrical particles.

One can estimate how realistic the obtained evaluations of hydrogen diffusivity D in uranium hydride are. Peretz et al. in Ref. [8] obtained about 80 kJ per mol. They explained that this high value results from diffusion mechanism via temperature activated vacancies. For this situation activation energy is the sum of the diffusion barrier height and the vacancy-formation energy. This explains why the diffusion through the hydride is much slower than through the metal. For this value (about 80 kJ per mol) we obtain 10^{-8} m^2 s^{-1} for the pre-exponent factor which is ''normal'' for such systems.

It is interesting that absorption by uranium (Table 4) for the last cycle is notably lower than that of the other cycles. This may be the result of accumulated contamination as mentioned in Ref. [6]. Our results confirm the presence of contamination that can slow the sorption down.

Note that fitted curves are comparable for both spherical and cylindrical shapes. It is not possible to give preference to one of these shape models. One of the reasons of this is small size of the particles so that diffusion is not rate-controlling. So the approximation hardly can be made better by considering other, less simple shapes. As soon as the real shape of the powder particles is very complex (see the SEM photo in Ref. [6]), this conclusion justifies using convenient simple symmetrical shapes such as sphere and cylinder.

Now, the obtained flux parameters shown in Tables 2–4 are discussed. Although absorption and desorption fluxes for UH_3 are much higher than the fluxes difference J_α for U, their difference J_β for UH_3 is much smaller than $J_\alpha = \text{const}$. In Fig. 6 one can see the ratio J_β/J_α with respect to time for the second cycle for both spheres (solid line) and cylinders (dashed line). The behaviour of the other cycles is similar. Note that even at the beginning, J_β is less than 10% with respect to J_α (the same for other cycles). During the skin growth stage the hydrogen concentration in UH_3 has equilibrium value and thus the ratio is constant. The calculation starts at the skin growth stage (nucleation stage is omitted).

Table 9 – Nucleation time t_λ (s)

Cycle no.	2	3	4	5	6	7	Many
Spheres	29.785	21.164	10.706	15.689	11.614	11.517	2.000
Cylinders	20.613	21.371	11.346	15.337	12.234	10.383	0

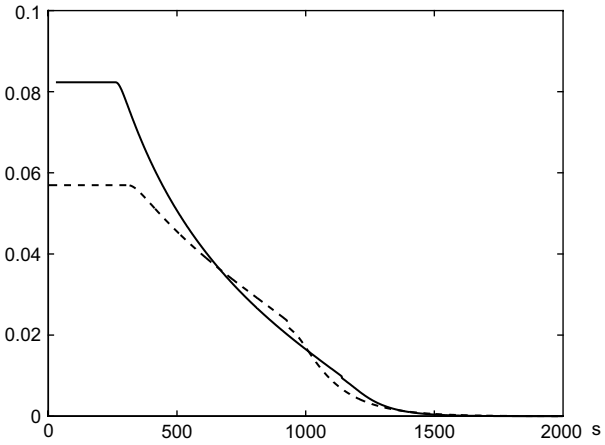

Fig. 6 – Ratio of the sorption fluxes by hydride and metal phase.

4. Summary

We presented a model that describes isothermal hydrogen sorption by uranium powder with hydride formation. Four consecutive stages of the process were considered: nucleation, skin development, skin growth, and final saturation. This allowed fitting the series of experimental curves (for consecutive cycles of hydriding) with low variance of parameters. The S-shape of the curves was explained by the nucleation stage.

Acknowledgements

The work has been financially supported by the programme ''Modern Numerical and Informational Technologies of Solving Large Problems'' of the Department of Mathematical Sciences of the Russian Academy of Sciences.

REFERENCES

[1] Sakintuna B, Lamari-Darkrim F, Hirscher M, Dogan B. Metal hydride materials for solid hydrogen storage: a review. Int J Hydrogen Energy 2007;32(9):1121–40.
[2] Martin M, Gommel C, Borkhart C, Fromm E. Absorption and desorption kinetics of hydrogen storage alloys. J Alloys Compd 1996;238:193–201.

[3] Schweppe F, Martin M, Fromm E. Model on hydride formation describing surface control, diffusion control and transition regions. J Alloys Compd 1997;261:254–8.
[4] Bloch J, Mintz MH. Kinetics and mechanisms of metal hydrides formation – a review. J Alloys Compd 1997;253–254:529–41.
[5] Bingert JF, Hanrahan Jr RJ, Field RD, Dickerson PO. Microtextural investigation of hydrided α-uranium. J Alloys Compd 2004;365:138–48.
[6] Bloch J. The hydriding kinetics of activated uranium powder under low (near equilibrium) hydrogen pressure. J Alloys Compd 2003;361:130–7.
[7] Fromm E, Gebhardt E. Gases and carbon in metals. Berlin: Springer-Verlag; 1976.
[8] Peretz M, Zamir D, Cinader G, Hadari Z. NMR study of hydrogen diffusion in uranium hydride. J Phys Chem Solids 1976;37(1):105–11.